

Hindawi Publishing Corporation
International Journal of Chemical Engineering
Volume 2010, Article ID 590169, 10 pages
doi:10.1155/2010/590169

Research Article

Performance Evaluation of AOP/Biological Hybrid System for Treatment of Recalcitrant Organic Compounds

Stanford S. Makgato¹ and Evans M. Nkhalambayausi-Chirwa²

¹Department of Chemical and Metallurgical Engineering, Faculty of Engineering and Built Environment, Tshwane University of Technology, Pretoria 0001, South Africa

²Water Utilization Division, Department of Chemical Engineering, University of Pretoria, Pretoria 0002, South Africa

Correspondence should be addressed to Evans M. Nkhalambayausi-Chirwa, evans.chirwa@up.ac.za

Received 23 December 2009; Accepted 7 April 2010

Academic Editor: Josiane Nikiema

Copyright © 2010 S. S. Makgato and E. M. Nkhalambayausi-Chirwa. This is an open access article distributed under the Creative Commons Attribution License, which permits unrestricted use, distribution, and reproduction in any medium, provided the original work is properly cited.

Process water from nuclear fuel recovery unit operations contains a variety of toxic organic compounds. The use of decontamination reagents such as CCl_4 together with phenolic tar results in wastewater with a high content of chlorophenols. In this study, the extent of dehalogenation of toxic aromatic compounds was evaluated using a photolytic advanced oxidation process (AOP) followed by biodegradation in the second stage. A hard-to-degrade toxic pollutant, 4-chlorophenol (4-CP), was used to represent a variety of recalcitrant aromatic pollutants in effluent from the nuclear industry. A UV-assisted AOP/bioreactor system demonstrated a great potential in treatment of nuclear process wastewater and this was indicated by high removal efficiency (> 98%) under various 4-CP concentrations. Adding hydrogen peroxide (H_2O_2) as a liquid catalyst further improved biodegradation rate but the effect was limited by the scavenging of OH^\bullet radicals under high concentrations of H_2O_2 .

1. Introduction

Process water from nuclear fuel recovery unit operations contains a variety of toxic organic compounds. The use of decontamination reagents such as CCl_4 together with phenolic tar results in wastewater with a high content of chlorophenols. Chlorophenols are compounds of serious environmental concern due to their toxic impacts and discharge from a wide range of industrial sources. A large number of chlorophenol derivatives are refractory in nature rendering them resistant to biological degradation. The recalcitrance of these compounds results from the carbon-hydrogen bond, which is cleaved with great difficulty [1]. Due to their stability, halogenated phenols tend to accumulate in higher-order organisms. In summary, a large component of nuclear waste contains organic waste consisting of alcohols and phenolics.

Current treatment processes for the removal of halogenated organic compounds involve dehalogenation using salts followed by chemical oxidation of the unhalogenated form [2]. The chemical process results in the production of harmful byproducts that require further disposal [3]. Among

the alternative methods to the chemical treatment processes are the biological processes using specialized species of chlorophenol degrading organisms, oxidative reaction using AOP and photocatalysis [4]. However, when used alone AOPs still produce harmful byproducts and may be energy intensive.

Lately, more interest has been directed towards finding solutions that involve the use of cultures of microorganisms to treat contaminated sediments and water impacted by nuclear waste [5]. The biological technology is the most cost effective alternative when compared to the other conventional treatment options as it has the potential to treat organic pollutants without leaving undesirable toxic byproducts. However, biological processes tend to be slow. A promising alternative is to use photoassisted AOP as a pre-treatment step to convert initially toxic organic compounds to more readily biodegradable intermediates followed by the biological oxidation of these intermediates to CO_2 and H_2O [3].

An example of an AOP/biological hybrid system is illustrated by Vogelpohl and Kim [6] in an experiment where naturally toxic compounds were detoxified in an AOP

thereby forming easily degradable compounds for further degradation in the biological process. In this study, the latter concept was evaluated for the treatment of nuclear process water using 4-CP as a primary carbon sources for a local mixed culture.

2. Materials and Methods

2.1. Microorganisms, Media, and Chemicals. A mixed culture of activated sludge bacteria was originally collected from sand drying beds at a nearby Wastewater Treatment Plant (WWTP) (Brits, Northwest Province). The start up culture was prepared by growing overnight in Luria-Bettani (LB) broth at 32°C. This culture was used to inoculate the biological reactor (2nd stage). The feed solution, basal mineral medium (BMM) was prepared by dissolving (in 1 L distilled water): 0.535 g NH_4Cl ; 10.744 g $\text{NaH}_2\text{PO}_4 \cdot 2\text{H}_2\text{O}$; 2.722 g K_2HPO_4 ; 0.0493 g $\text{MgSO}_4 \cdot 7\text{H}_2\text{O}$; 0.0114 g $\text{NaSO}_4 \cdot 2\text{H}_2\text{O}$; and 0.0493 g $\text{MgSO}_4 \cdot 3\text{H}_2\text{O}$. During the startup, 2 g L^{-1} of glucose was added to the feed solution in order to start the experiment with a healthy culture. The 4-CP used in this experiment was obtained at purities higher than 99% from MERCK Chemicals. LB agar was prepared by adding 20 g of agar powders in 1 L of distilled water. Plate Count Agar (PC) was prepared similarly. Both the LB Agar and PC Agar were autoclaved for 15 min and allowed to cool to 45°C before use.

2.2. Experimental Apparatus. The two-stage system used in this study consisted of a 22.8 L photoreaction chamber (Reactor 1) in Figure 1 followed by a 32.7 L biological reactor (Reactor 2) in Figure 1 both made from Perspex glass, 9 Watts UV-lamp, feed pump, and UV-recycle pump. The dimensions of the photoreactor were 300 × 295 × 295 mm (L × B × H) whereas the biological reactor were 447 × 348 × 246 mm (L × B × H). The two reactors were operated as CSTRs connected in series. Reactor 2 was expected to utilize byproducts of the degradation of phenolic compounds as carbon sources.

2.3. Culture Characterization. Phylogenetic characterization of cells was performed on individual colonies of bacteria from the 8th-10th tube in the tenfold serial dilution preparation. LB and Plate Count (PC) agar was used for colony development. In preparation for the 16S rRNA sequence identification, the colonies were first classified based on morphology. A 16S rRNA fingerprinting method was used to obtain DNA sequences of pure isolates from the sludge. Genomic DNA was extracted from the pure cultures using a DN easy tissue kit (QIAGEN Ltd, West Sussex, UK). 16S rRNA genes of the isolates were then amplified by reverse transcriptase-polymerase chain reaction (RT-PCR) using primers pA and pH1. The primer pA corresponds to position 8–27 and primer pH1 corresponds to position 1541–1522 of the 16S gene [7]. The PCR products were then sent to Inqaba Biotech facility (in Pretoria) for sequencing where an internal primer pD was used. Primer pD corresponds to position 519–536 of the 16S gene. The sequence relationships to known bacteria were determined by searching known

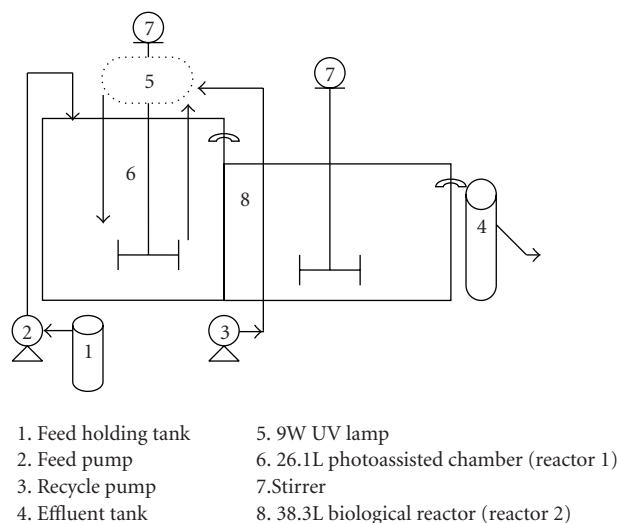


FIGURE 1: Apparatus set-up for photoassisted biodegradation process design.

sequences in GenBank using a basic BLAST search of the National Center for Biotechnology Information (NCBI) gene library.

2.4. Analytical Methods

2.4.1. Chlorophenol Determination. 4-CP concentration was measured in a Waters Alliance 2695 High-Performance Liquid Chromatography (HPLC) (Meadows Instrumentation Inc, Illinois, USA). The HPLC system consisted of the Waters 626 LC System, 717 Plus Autosampler, and the 996 Photodiode Array Detector. A Waters PAH C_{18} Symmetry Column (4.6 mm × 250 mm, 5 μm) was used. The samples were first filtered through a 5 mL syringe filter (0.4 5 μm pore size). The injection volume was 10 μL and the detector wavelength was 254 nm. The mobile phase used, A: B, 1% acetic acid in water: 1% acetic acid in acetonitrile. Data was interpreted by the Millennium 2010 Chromatography Manager.

2.4.2. Characterization of Intermediates. Degradation products were identified using gas chromatography coupled to mass spectrometry detector (GC-MS) (Clarus 600T, PerkinElmer, Massachusetts, USA) GC system with 5973N Mass Selective Detector, 7683 Series Injector Autosampler and G1701DA MSD Chem Station data acquisition software was used for GC-MS analysis. The GC separation was performed on a fused silica capillary column (30 m × 0.25 mm × 0.25 μm HP-5MS). The helium carrier gas flow rate was 1.0 mL min^{-1} ; the injector temperature was 250°C; the detector temperature was 280°C; and the transfer line temperature was set at 280°C. The column temperature was programmed to rise at a rate of 10°C min^{-1} first from 50 to 260°C, and then kept isothermal for 3 min at 260°C. 70 eV EI was used as the ionization voltage in the mass spectrometric analysis.

2.4.3. Gravimetric Analysis of Biomass. 2 mL of solution was drawn from the reactor and placed in preweighed centrifuged tube and centrifuged on Mini Spin (Eppendorf) for 10 min at 10,000 rpm. After decanting the supernatant, the wet centrifuged tube was weighed and placed into an oven at 50°C for 24 h. The resulting change in weight from dried centrifuged tube with biomass and without was used to determine the cell weight. The mass and the volume filtered were used to calculate suspended cells concentration in mg L^{-1} .

3. Reaction Rate Kinetics

A general mass balance of 4-CP around a completely mixed photoreactor is as follows [8]:

$$V \frac{dC}{dt} = Q(C_{\text{in}} - C) + r_s V, \quad (1)$$

where C_{in} = influent substrate concentration (ML^{-3}), C = effluent substrate concentration (ML^{-3}), reaction rate ($\text{ML}^{-3}\text{T}^{-1}$), Q is flow rate across the reactor (L^3T^{-1}), and V = operating volume of the reactor (L^3). During steady state operation, the left-hand derivative approaches zero, that is, $V \cdot dS/dt \Rightarrow 0$. Thus, (1) is simplified to.

$$-r_s = \left(\frac{Q}{V}\right)(C_{\text{in}} - C). \quad (2)$$

For the single reactant kinetics in the photochemical reaction chamber, we assume first-order rate kinetics, $-r_s = k_s \cdot C$, such that, the rate constant can be estimated during steady-state operation from the influent and effluent concentration as follows:

$$\frac{C}{C_{\text{in}}} = \frac{1}{1 + k_s \cdot \tau}, \quad (3)$$

where τ = the hydraulic retention time V/Q (T) and k_s = the first-order maximum reaction rate coefficient (T^{-1}).

For the biological reactor, two reaction rate models were evaluated—the reaction without inhibition as described by the Michaelis-Menten substrate utilization rate kinetics [9]:

$$-r_s = \frac{k_{ms}CX}{K_s + C} \quad (4)$$

and the reaction with substrate level inhibition as described by Briggs and Haldane [10]:

$$-r_s = \frac{k_{ms}CX}{K_s + C + C^2/K_I}, \quad (5)$$

where k_{ms} = maximum specific reaction rate coefficient (T^{-1}), K_s = half velocity concentration (ML^{-3}), K_I = coefficient of inhibition (ML^{-3}), and X = the viable cell concentration in the reactor (ML^{-3}). The reaction rate is substituted into the reactor mass balance as shown in (6) for example,

$$V \frac{dC}{dt} = Q(C_{\text{in}} - C) + \left(-\frac{k_{ms}C \cdot X}{K_s + C}\right)V \quad (6)$$

which resolves to

$$\frac{X\tau}{C_{\text{in}} - C} = \left(\frac{K_s}{k_{ms}}\right)\frac{1}{C} + \frac{1}{k_{ms}}. \quad (7)$$

Equation (7) determined from the cell mass balance across the reactor shows that the cell yield in the reactor is proportional to substrate utilized by bacteria in the reactor, that is, Y = mass of cells per mass of substrate utilized. The above expression is only true when the HRT is short enough such that cell death within the reactor is insignificant. Two operation conditions were required to yield two equations that were solved simultaneously for the parameters k_{ms} and K_s . The mass balance equation resulting from the substitution of the inhibition kinetics (5) is more complex

$$V \frac{dC}{dt} = Q(C_{\text{in}} - C) + \left(-\frac{k_{ms}C \cdot X}{K_s + C + C^2/K_I}\right)V \quad (8)$$

which resolves to

$$C_{\text{in}} - C = \left(\frac{V}{Q}\right)\left(-\frac{k_{ms}C \cdot X}{K_s + C + C^2/K_I}\right). \quad (9)$$

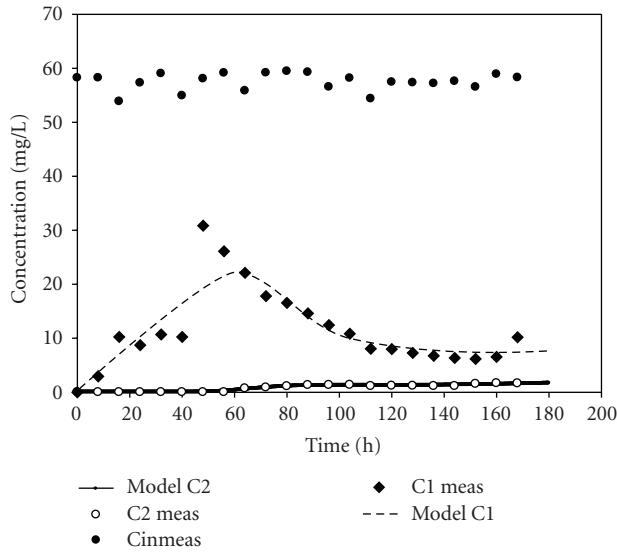
The above equation was solved numerically.

4. Results and Discussion

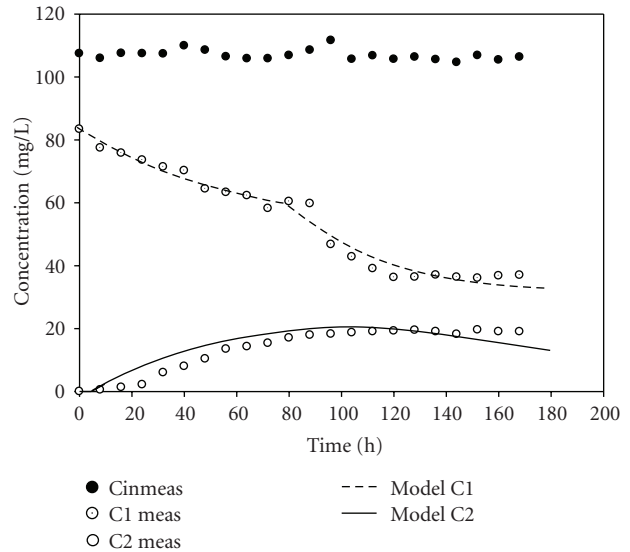
4.1. Effect of 4-Chlorophenol Influent Loading. A series of experiments were carried out at different feed 4-CP concentrations (50 to 1000 mg L^{-1}). The reactor was operated continuously until effluent conditions stabilized in a *quasi*-steady state. True steady-state conditions are expected after operation for 3 to 4 times the HRT (space times). This was shortened to two space times at a value of 6 days HRT. Operation at 50 mg L^{-1} yielded *quasi*-steady state conditions with observed effluent concentrations of 6.24 mg 4-CP L^{-1} in the chemical reactor and 1.13 mg 4-CP L^{-1} in the biological reactors (Figure 2(a)). Operation at 100 mg L^{-1} yielded *quasi* steady-state conditions with observed effluent concentrations of 36.3 mg 4-CP L^{-1} in the chemical reactor and 19.2 mg 4-CP L^{-1} in the biological reactor (Figure 3(a)).

The system was further challenged to 4-CP concentration of 200 mg L^{-1} . At the latter concentration, no *quasi*-steady state was attained and was characterized by significant viable biomass losses. The system was further challenged with an influent of 1000 mg L^{-1} . No *quasi*-steady state was attained under this loading due to high toxicity and loss of biomass (Figure 4). The results show that it was necessary to keep the 4-CP influent to the second stage very low for the biological system to function properly.

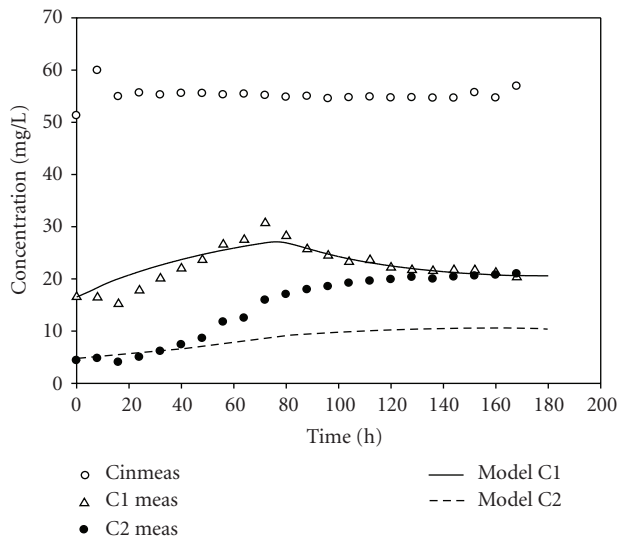
4.2. Effect of H_2O_2 in the Influent Concentration. Another important parameter to consider in the combined AOPs with biological treatment process is the amount of H_2O_2 required to obtain the best efficiency in the treatment. The impact of adding the chemical catalyst H_2O_2 was investigated within the loading range (50 to 300 mg L^{-1}) using an H_2O_2 dose of 0.1 mL L^{-1} . The effect of H_2O_2 on the removal of 4-CP is shown in Figures 2(b), 3(b) and 5.



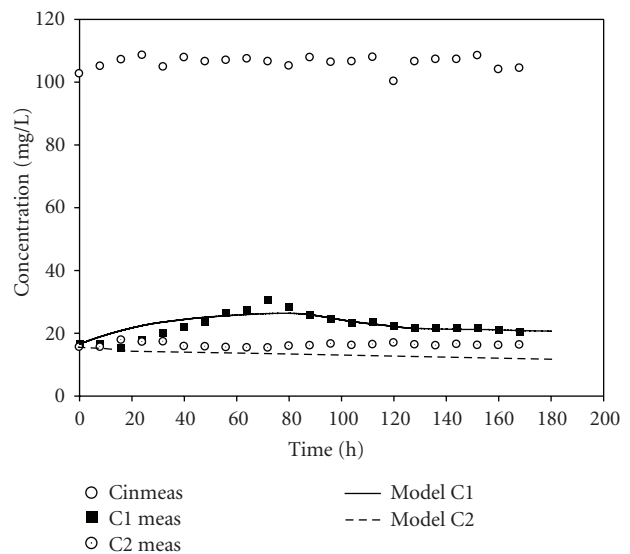
(a)



(a)



(b)



(b)

FIGURE 2: Photodegradation and biodegradation of 4-CP at an influent of 50 mg L^{-1} (a) Without H_2O_2 , (b) With H_2O_2 .

FIGURE 3: Photodegradation and biodegradation of 4-CP at an influent of 100 mg L^{-1} (a) Without H_2O_2 , (b) With H_2O_2 .

When $0.1 \text{ mL H}_2\text{O}_2 \text{ L}^{-1}$ was added into $50 \text{ mg 4-CP L}^{-1}$ influent, *quasi-steady state* was attained for both the chemical reactor ($21.6 \text{ mg 4-CP L}^{-1}$) and biological reactor ($19.8 \text{ mg 4-CP L}^{-1}$) resulting in effluent concentration of 21.72 . Operation with added H_2O_2 under an influent 4-CP concentration of $100 \text{ mg 4-CP L}^{-1}$ resulted in *quasi-steady state* conditions at effluent concentrations of $21.3 \text{ mg 4-CP L}^{-1}$ in the chemical chamber and $16.9 \text{ mg 4-CP L}^{-1}$ in the biological reactor.

At $200 \text{ mg 4-CP L}^{-1}$ the system reached *quasi-steady-state* conditions with 10.1 mg L^{-1} in the chemical reactor and 6.6 mg L^{-1} in the biological reactor (Figure 5). These results show that, adding the chemical catalyst (H_2O_2) improved the performance of the system with much lower concentrations observed in both the chemical and biological reactors. This

is in comparison with performance at $200 \text{ mg 4-CP L}^{-1}$ influent concentration whereby there was significant viable biomass loss before *quasi-steady-state* conditions could be reached. The results agree with the reported results by Wen et al. [11] in which 4-CP concentration was tested at initial concentrations higher than 300 mg L^{-1} in bioreactors operated under aerobic and anaerobic conditions.

The system was further challenged with 4-CP influent concentration of 300 mg L^{-1} in the presence of $0.1 \text{ mL H}_2\text{O}_2 \text{ L}^{-1}$. The system did not attain *quasi-steady-state* condition. This was accompanied by excessive loss of viable biomass.

The above data in the peroxide experiment show that, 4-CP degradation in the photoreactor was highest at 200 mg L^{-1} indicating an optimum operation condition at this concentration. The suggestions by Pera-Titus et al.

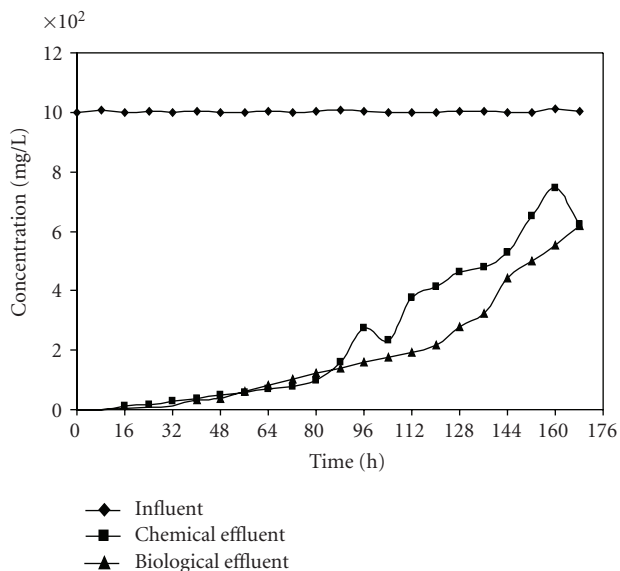


FIGURE 4: Photodegradation and biodegradation of 4-CP at an influent of 1000 mg L^{-1} without H_2O_2 .

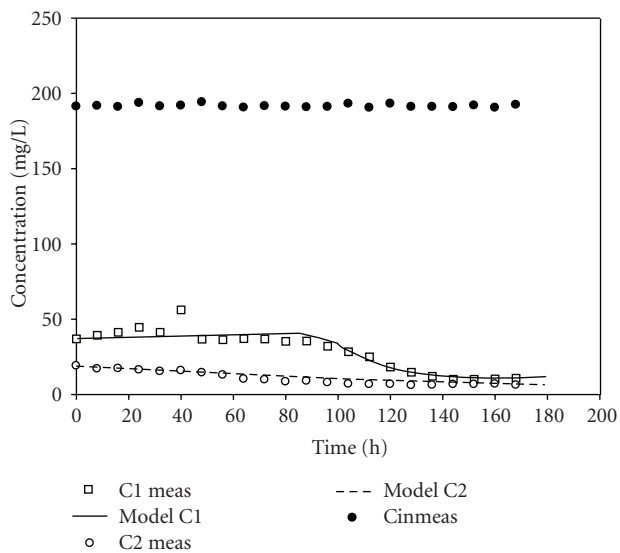
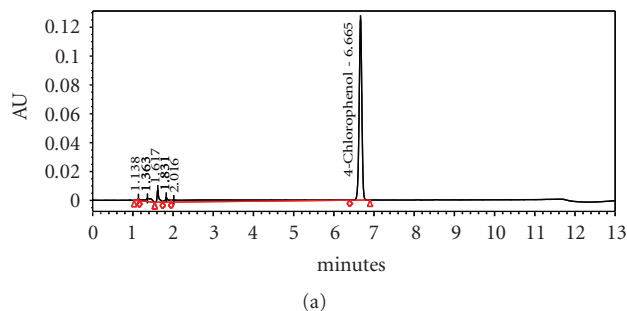


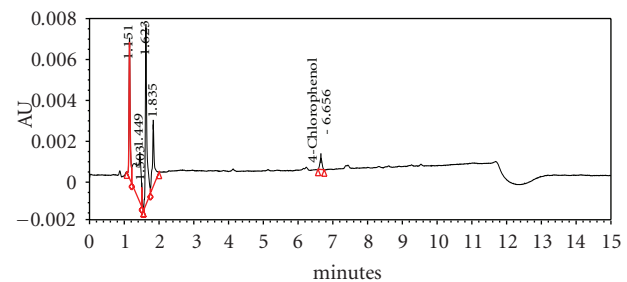
FIGURE 5: Photodegradation and biodegradation of 4-CP at an influent of 200 mg L^{-1} with H_2O_2 .

[12] that the existence of an excessive amount of non-reacted OH^\bullet radicals under a low organic feed results in the recombination of the radicals to form water without useful reaction with the organics was confirmed.

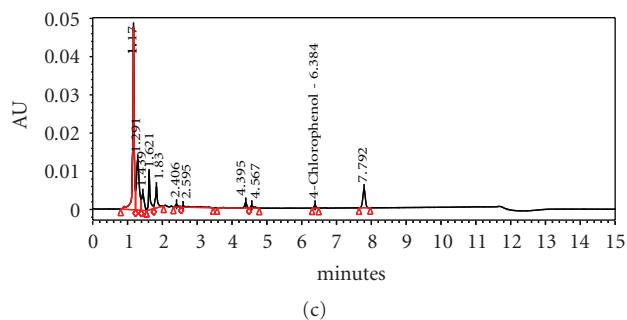
The above is supported by another case reported by Xu et al. [13] where the enhancement of degradation by addition of H_2O_2 was due to the increase in the (OH^\bullet) radical concentration. Our results are in good agreement with Wen et al. [11] findings who reported that direct photolysis appears to be less effective than other processes where radiation is combined with H_2O_2 or O_3 , or where homogeneous, heterogeneous catalysis or photocatalysis are employed.



(a)



(b)



(c)

FIGURE 6: Chromatographic showing residual (a) 4-chlorophenol (b) Intermediates, (c) Metabolites [16].

4.3. 4-Chlorophenol Removal Efficiency. The removal efficiency of 4-CP was calculated from experimental data and the results were recorded over a range of concentration as indicated in Table 1. These results agree with cited results by various literature reports [14, 15] where authors examined the efficiency of the combined photochemical and biological treatment process. When the influent concentration was doubled without changing any of the process parameters to 100 mg L^{-1} , the overall percentage degradation of 82% was observed. Sahinkaya and Dilek [15] obtained 98% when using 100 mg L^{-1} with added TiO_2 as a catalyst. When combine UV assisted AOP with biological treatment process was challenged to 200 mg L^{-1} , no quasi-steady-state was obtained in the biological reactor due to significant loss of viable biomass. It could be seen from the observed results that the degradation efficiency was affected by increase in influent concentration.

In another example, Suryaman [14] used combined biological-photocatalytic treatment process to treat wastewater containing phenol at 50 mg L^{-1} . The results from the latter study indicated that phenol was removed to the concentration of 6.8 mg L^{-1} . It can therefore be deduced that

TABLE 1: Summary of combined photoassisted AOPs with biological treatment process performance.

No	Influent (4-CP) concentration	UV-AOP removal (%)	Biological removal (%)	Combined process (%)
1	50 mg L ⁻¹	89.2	83.1	98
2	100 mg L ⁻¹	65.2	48.6	82.2
3	200 mg L ⁻¹	—	—	—
4	1000 mg L ⁻¹	—	—	—
5	50 mg L ⁻¹ with 0.1 ml H ₂ O ₂ L ⁻¹	62.5	2.2	63
6	100 mg L ⁻¹ with 0.1 ml H ₂ O ₂ L ⁻¹	79.9	25.3	85
7	200 mg L ⁻¹ with 0.1 ml H ₂ O ₂ L ⁻¹	94.6	33.9	96.4
8	300 mg L ⁻¹ with 0.1 ml H ₂ O ₂ L ⁻¹	—	—	—

“—” means no *quasi*-steady-state was reached.

TABLE 2: Characterized activated sludge cultures.

No	Blast result	Max ID	Further down on list (same max ID)
1	Uncultured bacterium, <i>Delftia</i> spp	99%	<i>Delftia tsuruhatensis</i>
2	<i>Staphylococcus pasteurii</i>	99%	<i>Deinococcus</i> spp.
3	<i>Bacillales</i> bacterium, <i>S. pasteurii</i>	99%	
4	<i>Pseudomonas stutzeri</i>	100%	Other <i>Pseudomonas</i> spp. (99%)
5	<i>Stenotrophomonas maltophilia</i>	100%	<i>P. aeruginosa</i> (99%)
6	<i>B. cereus</i>	100%	<i>B. thuringiensis</i> (99%)
7	<i>Pseudomonas mendocina</i>	100%	Other <i>Pseudomonas</i> spp. (99%)
8	<i>Pseudomonas lubricans</i>	99%	Other <i>Pseudomonas</i> spp.
9	Uncultured Caulobacteraceae	100%	<i>Brevundimonas</i> spp.
10	<i>P. aeruginosa</i>	99%	Other <i>Pseudomonas</i> spp.

the removal rate in the current culture is much higher both with and without chemical catalyst (H₂O₂). In this study, the highest removal efficiencies of 4-CP were obtained at 50 mg L⁻¹ and 200 mg L⁻¹ with added H₂O₂ (98.0% and 96.4%, resp.) (Table 1). The lowest 4-CP removal efficiency was obtained at 50 mg L⁻¹ with added H₂O₂. In all cases, 4-CP was not completely removed in the bioreactor meaning that concentration of 4-CP could still be detected in low concentrations.

4.4. Identification of Intermediates and Metabolites. Figure 6 is a chromatogram showing residual 4-chlorophenol (a), intermediates (b) and metabolites (c) as shown by HPLC, [16]. It could be seen from the figure how the 4-CP disappears from chemical reactor to biological reactor. Ten different intermediates were detected by GC-MS.

In various studies, different authors [17–20] examined the reaction pathway for the 4-CP oxidation. The results of extensive research conducted by various researchers listed the main intermediates products of 4-CP as: benzoquinone, hydroquinone, 4-chlorocatechol; and chlorohydroxyquinol. The main intermediates found in this study are not in agreement with these reported primary oxidation products of 4-CP. However, 1,2 benzenedicarboxylic acid, propanoic acid, hexadecanoic acid in Table 2 agrees with the results reported by [21–23]. Various authors, [24, 25] also confirmed that more organic acids could be formed as more 4-CP degraded. In a separate report, Ying et al. [26] also agreed that organic acids such as formic, acetic, oxalic, propanoic and maleic

acid were generated in 4-CP degradation process. 2-(3,5-dichloro-4-methoxymethylphenyl) also agrees with results reported by Theurich et al. [27] where biphenyl derivatives were reported as 4-CP degradation products.

Different types of photoproducts and metabolites have been identified both in this study and in the literature. According to Arslan-Alaton et al. [28], the major concerns of organic pollutants degradation by AOPs is the nature of oxidation intermediates and end products. Equally important, Lipczynska-Kochany and Bolton [29] mentioned that treatment products might be more toxic or recalcitrant than the original pollutants after being subjected to advanced oxidation. As a result, it was of paramount importance to qualitatively identify degradation products in order to suggest a reaction mechanism.

In order to avoid high energy consumption which represents about 60% of the total operational cost because of the electric light sources, the photolytic treatment time must be reasonably short. However, if the fixed pretreatment time is too short, the intermediates remaining in the solution could still be structurally similar to the initial biorecalcitrant compounds and therefore non-biodegradable, [3].

4.5. Culture Characterization. Using 16S rRNA fingerprint, ten species of bacteria including *Staphylococcus pasteurii*, *Bacillales* bacterium, *Pseudomonas stutzeri*, *Stenotrophomonas maltophilia*, *Bacillus cereus*, *Delftia* spp., *Pseudomonas mendocina*, *Pseudomonas lubricans*, *Caulobacteraceae* spp., and *Pseudomonas aeruginosa* were characterized as shown in

TABLE 3: Chemical reactor reaction rate coefficients

Targeted concentration (mg L ⁻¹)	50	100	200	50 + H ₂ O ₂	100 + H ₂ O ₂	200 + H ₂ O ₂
Observed concentration (mg L ⁻¹)	55	107	205	55	106	191
Steady-state concentration (mg L ⁻¹)	6.24	36.2	—	21.6	21.3	10.1
k_s (h ⁻¹)	0.070	0.017	—	0.014	0.035	0.157

“—” means no quasi-steady-state was reached.

TABLE 4: Operating conditions for 2nd stage biological reactor.

Parameter	50 mg L ⁻¹	100 mg L ⁻¹	200 mg L ⁻¹
	With 0.1 ml H ₂ O ₂	With 0.1 ml H ₂ O ₂	With 0.1 ml H ₂ O ₂
C_{in} (mg L ⁻¹)	21	36	10
C (mg L ⁻¹)	20	19	6
V (L)	32.7	32.7	32.7
Q (L h ⁻¹)	0.20	0.20	0.20
X_0 (g m ⁻³)	52	44	37
Weight of 1 ml of cells (g)	45×10^{-4}	45×10^{-4}	45×10^{-4}

Table 2. Among the identified species, the two *Pseudomonas* species, *P. aeruginosa* and *P. mendocina* are well known aromatic compound degraders. *P. mendocina* has been demonstrated to degrade toluene at the laboratory scale where as *P. aeruginosa* has been extensively studied in the degradation of chlorophenols and other polynuclear aromatic compounds, [30]. Other species such as *P. stutzeri* are capable of degrading aliphatic chlorinated compounds such as carbon tetrachloride, [30]. These species could serve as house keeping organisms by degrading halogenated byproducts of chlorophenol degradation in the biological reactor. These results are in good agreement with Field and Sierra-Alvarez [31] who also reported that *Pseudomonas sp B-13* are capable of growing on 4-CP as a source of carbon and energy.

5. Parameter Evaluation

5.1. Parameter Evaluation in the Chemical Reactor. The photochemical reactor reaction rate coefficient was calculated using (3) and the values are recorded as indicated in Table 3. From Table 3 above, it could be concluded that increasing the influent concentration of 4-CP while maintaining H₂O₂ concentration negatively affected the first-order reaction rate constant, k . The findings published by Catalkaya et al. [32] were compared with the calculated k_s values in this study. Catalkaya et al. [32] reported k_s values as 0.0997, 0.0480 and 0.0307 for 50, 100 and 200 mg L⁻¹ with added H₂O₂, respectively. The difference between the literature values and the values obtained in this study are attributed to difference in experimental conditions employed. The pseudo-first order rate constants (k_s) of 4-CP with (OH[•]) radicals was also reported in another case by Ghaly et al. [33] as 0.15 min⁻¹. The result of Ghaly et al. [33] appears to be too high in comparison to our observed k values partly due to the fact

that Ghaly et al. [33] used the light intensity of 60 W, seven times higher than the 9 W used in this study.

5.2. Steady-State Estimation of Biological Parameters. The values of the kinetic parameters, K_s , k_{ms} and K_I in the continuous flow process were determined from the experimental data under quasi-steady-state conditions as shown in Table 4 using (7) and (9). The values are recorded in Table 5. The degradation rate coefficient, k_{ms} , was determined to be very low compared to first-order maximum reaction rate coefficients, k as shown in Table 3. The low value of k_{ms} is a result of the low 4-CP loading at the HRT of 6 days. Maximum specific reaction rate coefficient in the biological reactor, k_{ms} is lower than the chemical reactor first-order maximum reaction rate coefficient, k_s . This indicates that 4-CP was degraded faster in the chemical reactor than in the biological reactor. In addition, the inhibition effects (K_I) of 4-CP biodegradation was found to be 25.0 mg L⁻¹. The K_I value is in good range reported by Konya et al. [34] as shown in Table 5. The high value of K_I also implies that the inhibition was very high which means that the bacteria were probably growing predominantly on the 4-CP intermediates.

5.3. Parameter Estimation Using Transient State Model. Since the reactor were operated 2-3 HRTs each, true steady state conditions could not have been reached. For a more realistic modeling effort, the reaction rates kinetics were evaluated under transient state using the Aquatic systems Simulation software (AQUASIM 2.0). In AQUASIM 2.0, the mass balance (2) and (6) were evaluated numerically by fourth order Runge-Kutta method (RK-4). The parameters were obtained by minimizing the Chi-square (χ^2) values between the model data and the actual data using a simplex method built within AQUASIM, [35].

The parameters derived from the steady-state assumptions for the chemical reactor did not fit the experimental data because it did not take into consideration the accumulation of the H₂O₂, catalyst in the system. During photolytic degradation, the amount of (OH[•]) radical formation is the driving force for 4-CP removal. The (OH[•]) radical started accumulating in Reactor 1 only after the UV light was switched on. At the beginning of each run, the (OH[•]) radical was not sufficient to facilitate 4-CP removal. This resulted in the characteristic rise and deep in the 4-CP concentration in Reactor 1. In order to capture this trend, changes are proposed in the following model:

- (1) Since the (OH[•]) radical is the second reactant, the reaction is adjusted to the second order with respect to 4-CP and (OH[•]) radical.

TABLE 5: Parameter estimation in biological reactor using numerical methods.

Parameter	Units	Experimental results		Results from literature	
		(Michaelis-Menten model) Value	(Haldane Model) Value	Konya et al. [34]	Jiang et al. [36]
Microorganisms used		Activated sludge	Activated sludge	Activated sludge	<i>Candida tropicalis</i>
K_s	mg L ⁻¹	18.95	4.59	25.7	1.11 × 10 ³
k_{ms}	h ⁻¹	6.091 × 10 ⁻⁶	3.43 × 10 ⁻⁶	0.06	4.79
K_I	mg L ⁻¹	—	25.0	17.0	4.33

—: means not applicable.

- (2) Logistic accumulation of the (OH•) radical is suggested to capture the rising trend in the reaction rate.
- (3) The occurrence of the (OH•) radical in solution is transitional.

The revising of the first-order rate kinetics $-r_s = k_s \cdot C$ with consideration for the concentration of the (OH•) radical required for initial 4-CP removal followed second-order rate kinetics, (10).

$$r_1 = kC_1C_{oh}, \quad (10)$$

where:

$$C_{oh} = C_{ohmax} + \frac{a}{[1 + e^{-(t-t_0)/b}]} c, \quad (11)$$

$$X = X_0 e^{(Yk_{ms}C_2/K_s - k_d)t}$$

5.3.1. Chemical Reactor Parameters. Estimated kinetic parameters for the chemical reactor are presented over a range of influent concentration as: $a = 648.78 \text{ mg L}^{-1}$, $b = 14.27 \text{ h}^{-1}$, $c = 249.39$, $t_0 = 10.13 \text{ h}$, $k = 1.97 \times 10^{-5} \text{ L}^{-3} \text{ mg}^{-1} \text{ h}^{-1}$, $C_{ohmax} = 534.82 \text{ mg L}^{-1}$ and $\chi^2 = 1046.55$. These kinetic parameters were determined by means of optimization.

5.3.2. Biological Reactor Parameters. The average kinetic parameters in the biological reactor were determined for both inhibited and non-inhibited conditions: $k_d = 2.02 \times 10^{14} \text{ (h}^{-1}\text{)}$, $K_s = 3.24 \times 10^{-4} \text{ mg L}^{-1}$, $X_0 = 1740 \text{ mg L}^{-1}$ and $\chi^2 = 921.52$ and with inhibition: $k_d = 2.00 \times 10^{14} \text{ (h}^{-1}\text{)}$, $K_I = 259.01 \text{ mg L}^{-1}$, $k_{ms} = 1.96 \times 10^{-5} \text{ h}^{-1}$, $K_s = 3.24 \times 10^{-4} \text{ mg L}^{-1}$, $X_0 = 908 \text{ mg L}^{-1}$, and $\chi^2 = 921.52$. These parameters values were adjusted by reoptimization against measured data.

5.4. Model Validation. Model predictions were in good agreement with the experimental data indicating the validity of the model (Figures 2(a), 3(a), 3(b), and 4). However, in Figure 2(b), the proposed model could not track the 4-CP concentration profiles. The effluent concentrations of 21 mg L^{-1} in the chemical reactor and 20.5 mg L^{-1} in the biological reactor were recorded at quasi-steady-state resulting in poor biodegradation efficiency of 2.2%, (Table 1). The difference between these values is insignificant and thus makes the model to not work well because of poor degradation efficiency. Therefore low efficiency limits

applicability of the model on photoassisted AOPs with biological treatment process.

The estimated parameters may be valid for the wastewater containing 4-CP and other chlorinated mono-nuclear phenols. Obtained results in this study are sufficient to promote combined photoassisted AOPs with biological treatment process for treatment of organic pollutants in nuclear industry applications.

6. Conclusion

In this study, a combined AOP with biological treatment process (hybrid reaction process) was applied to treat halogenated breakdown products from nuclear fuel recovery process water. Based on the experimental results, the following conclusions can be drawn: (1) a mixed culture of microorganism isolated from sand drying beds at a nearby wastewater treatment plant (Brits, Northwest Province) completely degraded 4-CP to a maximum concentration of 100 mg L^{-1} ; (2) adding hydrogen peroxide (H_2O_2) as a liquid catalyst further improved biodegradation rate but the effect was limited by the scavenging of OH• radicals under high concentrations of H_2O_2 . In fact the AOP step was able to enhance the capacity of removing 4-CP and practically mineralizing the organic matter in the biological treatment stage. A combined Advanced Oxidation Processes with biological treatment and UV/ H_2O_2 processes were thus demonstrated to be a feasible method to efficiently remove 4-CP from the aqueous phase.

Nomenclature

- a : kinetic parameter for accumulation of hydroxide radical (ML^{-3})
- b : kinetic parameter for accumulation of hydroxide radical (T)
- c : kinetic parameter for accumulation of hydroxide radical
- C : concentration at steady-state (ML^{-3})
- C_1 : chemical reactor calculated effluent concentration (ML^{-3})
- $C_{1\text{meas}}$: chemical reactor measured effluent concentration (ML^{-3})
- C_2 : biological reactor calculated effluent concentration (ML^{-3})
- $C_{2\text{meas}}$: biological reactor measured effluent concentration (ML^{-3})

C_{in} :	influent substrate concentration (ML^{-3})
C_{inmeas} :	influent measured substrate concentration (ML^{-3})
C_{oh} :	calculated concentration of hydroxyl radical (ML^{-3})
C_{ohmax} :	initial concentration of hydroxyl radical (ML^{-3})
C_{ohmeas} :	concentration of hydroxyl radical from literature (ML^{-3})
k_s :	the first-order maximum reaction rate coefficient (T^{-1})
k :	the second-order maximum reaction rate coefficient ($L^3M^{-1}T^{-1}$)
k_d :	endogenous decay coefficient (T^{-1})
K_i :	coefficient of inhibition (ML^3)
k_{ms} :	maximum specific reaction rate coefficient (T^{-1})
K_s :	half velocity concentration (ML^{-3})
Q :	flow rate across the reactor (L^3T^{-1})
r_1 :	the rate of 4-CP degradation in chemical reactor (T^{-1})
r_2 :	the rate of 4-CP biodegradation in biological reactor (T^{-1})
r_s :	reaction rate for substrate s ($T^{-1}ML^{-3}$)
τ :	the hydraulic retention time (T)
t :	time (T)
t_0 :	initial boundary value for accumulation of hydroxide radicals (T)
V :	reactor volume (L^3)
X :	viable cells concentration in the reactor (ML^{-3})
X_0 :	initial viable cells concentration in the reactor (ML^{-3})
χ^2 :	chi squared
X_s :	cell concentration in reactor at steady-state (ML^{-3})

Acknowledgment

The research was conducted as part of the exploratory research on the Biological Treatment of Radioactive Waste funded by the South African National Research Foundation (NRF) through the Grant no. FA2007030400002 awarded to Professor Evans M. N. Chirwa of the University of Pretoria.

References

- [1] H. Movahedyan, A. Assadi, and M. M. Amin, "Effects of 4-chlorophenol loadings on acclimation of biomass with optimized fixed time sequencing batch reactor," *Iranian Journal of Environmental Health, Science and Engineering*, vol. 5, no. 4, pp. 225–234, 2008.
- [2] J. E. T. van Hylckama Vlieg and D. B. Janssen, "Formation and detoxification of reactive intermediates in the metabolism of chlorinated ethenes," *Journal of Biotechnology*, vol. 85, no. 2, pp. 81–102, 2001.
- [3] V. Sarria, M. Deront, P. Perinnger, and C. Pulgarin, "Degradation of a biorecalcitrant dye precursor present in industrial wastewaters by a new integrated iron(III) photoassisted-biological treatment," *Applied Catalysis B*, vol. 40, no. 3, pp. 231–246, 2003.
- [4] H. Kušić, N. Koprivanac, A. L. Božić, and I. Selanec, "Photo-assisted Fenton type processes for the degradation of phenol: a kinetic study," *Journal of Hazardous Materials*, vol. 136, no. 3, pp. 632–644, 2006.
- [5] T. Barkay and J. Schaefer, "Metal and radionuclide bioremediation: issues, considerations and potentials," *Current Opinion in Microbiology*, vol. 4, no. 3, pp. 318–323, 2001.
- [6] A. Vogelpohl and S.-M. Kim, "Advanced oxidation processes (AOPS) in wastewater treatment," *Journal of Industrial and Engineering Chemistry*, vol. 10, no. 1, pp. 33–40, 2004.
- [7] T. Coenye, E. Falsen, M. Vancanneyt, et al., "Classification of *Alcaligenes faecalis*-like isolates from the environment and human clinical samples as *Ralstonia gilardii* sp. nov.," *International Journal of Systematic Bacteriology*, vol. 49, no. 2, pp. 405–413, 1999.
- [8] E. Metcalf, *Wastewater Engineering: Treatment and Reuse*, McGraw-Hill, Boston, Mass, USA, 4th edition, 2003.
- [9] S. Pallerla and R. P. Chambers, "Reactor development for biodegradation of pentachlorophenol," *Catalysis Today*, vol. 40, no. 1, pp. 103–111, 1998.
- [10] G. E. Briggs and J. B. Haldane, "A note on the kinetics of enzyme action," *Biochemical Journal*, vol. 19, no. 2, pp. 338–339, 1925.
- [11] J. Wen, H. Li, J. Bai, and Y. Jiang, "Biodegradation of 4-chlorophenol by *Candida albicans* PDY-07 under anaerobic conditions," *Chinese Journal of Chemical Engineering*, vol. 14, no. 6, pp. 790–795, 2006.
- [12] M. Pera-Titus, V. García-Molina, M. A. Baños, J. Giménez, and S. Esplugas, "Degradation of chlorophenols by means of advanced oxidation processes: a general review," *Applied Catalysis B*, vol. 47, no. 4, pp. 219–256, 2004.
- [13] B. Xu, N.-Y. Gao, X.-F. Sun, et al., "Photochemical degradation of diethyl phthalate with UV/H₂O₂," *Journal of Hazardous Materials*, vol. 139, no. 1, pp. 132–139, 2007.
- [14] D. Suryaman, K. Hasegawa, and S. Kagaya, "Combined biological and photocatalytic treatment for the mineralization of phenol in water," *Chemosphere*, vol. 65, no. 11, pp. 2502–2506, 2006.
- [15] E. Sahinkaya and F. B. Dilek, "Modeling chlorophenols degradations in sequencing batch reactors with instantaneous feed-effect of 2,4 DCP presences on 4-CP degradation kinetics," *Biodegradation*, vol. 18, pp. 427–437, 2007.
- [16] S. S. Makgato and E. M. N. Chirwa, "Photoassisted biodegradation of halogenated breakdown products in nuclear fuel recovery process water—hybrid reaction process," *Chemical Engineering Transactions*, vol. 17, pp. 1167–1172, 2009.
- [17] E. Brillas, C. Arias, P. L. Cabot, F. Centellas, J. A. Garrido, and M. Dodriguez, "Degradation of organic contaminants by advanced electrochemical oxidation methods," *Portugaliae Electrochimica Acta*, vol. 24, pp. 159–189, 2006.
- [18] Y. Cheng, H. Sun, W. Jin, and N. Xu, "Photocatalytic degradation of 4-chlorophenol with combustion synthesized TiO₂ under visible light irradiation," *Chemical Engineering Journal*, vol. 128, no. 2-3, pp. 127–133, 2007.
- [19] U. I. Gaya and A. H. Abdullah, "Heterogeneous photocatalytic degradation of organic contaminants over titanium dioxide: a review of fundamentals, progress and problems," *Journal of Photochemistry and Photobiology C*, vol. 9, no. 1, pp. 1–12, 2008.

- [20] X. L. Hao, M. H. Zhou, and L. C. Lei, "Non-thermal plasma-induced photocatalytic degradation of 4-chlorophenol in water," *Journal of Hazardous Materials*, vol. 141, no. 3, pp. 475–482, 2007.
- [21] R. J. A. L'Amour, E. B. Azevedo, S. G. F. Leite, and M. Dezotti, "Removal of phenol in high salinity media by a hybrid process (activated sludge + photocatalysis)," *Separation and Purification Technology*, vol. 60, no. 2, pp. 142–146, 2008.
- [22] H. Wang and J. Wang, "Electrochemical degradation of 4-chlorophenol using a novel Pd/C gas-diffusion electrode," *Applied Catalysis B*, vol. 77, no. 1-2, pp. 58–65, 2007.
- [23] Y. Zhang, M. Zhou, X. Hao, and L. Lei, "Degradation mechanisms of 4-chlorophenol in a novel gas-liquid hybrid discharge reactor by pulsed high voltage system with oxygen or nitrogen bubbling," *Chemosphere*, vol. 67, no. 4, pp. 702–711, 2007.
- [24] X. Li, J. W. Cubbage, and W. S. Jenks, "Photocatalytic degradation of 4-chlorophenol," *Journal of Organic Chemistry*, vol. 64, no. 23, pp. 8525–8536, 1999.
- [25] Ch. M. Du, J. H. Yan, and B. G. Cheron, "Degradation of 4-chlorophenol using a gas-liquid gliding arc discharge plasma reactor," *Plasma Chemistry and Plasma Processing*, vol. 27, no. 5, pp. 635–646, 2007.
- [26] X. Yin, W. Bian, and J. Shi, "4-chlorophenol degradation by pulsed high voltage discharge coupling internal electrolysis," *Journal of Hazardous Materials*, vol. 166, no. 2-3, pp. 1474–1479, 2009.
- [27] J. Theurich, M. Lindner, and D. W. Bahnemann, "Photocatalytic degradation of 4-chlorophenol in aerated aqueous titanium dioxide suspensions: a kinetic and mechanistic study," *Langmuir*, vol. 12, no. 26, pp. 6368–6376, 1996.
- [28] I. Arslan-Alaton, T. Olmez-Hanci, B. H. Gursoy, and G. Tureli, "H₂O₂/UV-C treatment of the commercially important aryl sulfonates H-, K-, J-acid and Para base: assessment of photodegradation kinetics and products," *Chemosphere*, vol. 76, no. 5, pp. 587–594, 2009.
- [29] E. Lipczynska-Kochany and J. R. Bolton, "Flash photolysis/HPLC method for studying the sequence of photochemical reactions: applications to 4-chlorophenol in aerated aqueous solution," *Journal of Photochemistry and Photobiology A*, vol. 58, no. 3, pp. 315–322, 1991.
- [30] W. Gaofeng, X. Hong, and J. Mei, "Biodegradation of chlorophenols: a review," *Chemical Journal on Internet*, vol. 6, no. 10, pp. 1–67, 2004.
- [31] J. A. Field and R. Sierra-Alvarez, "Microbial degradation of chlorinated phenols," *Reviews in Environmental Science and Biotechnology*, vol. 7, no. 3, pp. 211–241, 2008.
- [32] E. C. Catalkaya, U. Bali, and F. Sengiil, "Photochemical degradation and mineralization of 4-chlorophenol," *Environmental Science and Pollution Research*, vol. 10, no. 2, pp. 113–120, 2003.
- [33] M. Y. Ghaly, G. Hartel, R. Mayer, and R. Haseneder, "Photochemical oxidation of p-chlorophenol by UV/H₂O₂ and photo-Fenton process. A comparative study," *Waste Management*, vol. 21, no. 1, pp. 41–47, 2001.
- [34] I. Konya, S. Eker, and F. Kargi, "Mathematical modelling of 4-chlorophenol inhibition on COD and 4-chlorophenol removals in an activated sludge unit," *Journal of Hazardous Materials*, vol. 143, no. 1-2, pp. 233–239, 2007.
- [35] P. Rechert, *Computer Program for the Identification and Simulation of Aquatic Systems—AQUASIM 2.0: User Manual*, Swiss Federal Institute for Environmental Science and Technology (EAWAG), Dübendorf, Switzerland, 1998.
- [36] Y. Jiang, J. Wen, L. Lan, and Z. Hu, "Biodegradation of phenol and 4-chlorophenol by the yeast *Candida tropicalis*," *Biodegradation*, vol. 18, no. 6, pp. 719–729, 2007.



Hindawi

Submit your manuscripts at
<http://www.hindawi.com>

